14C.3

Climatological depiction of hurricane structure from passive microwave and scatterometer observations: Using the 12-year JPL Tropical Cyclone Information System (TCIS) to create composites and establish reliable statistics.

Svetla Hristova-Veleva[1], Bryan Stiles[1], Tsae-Pyng Shen[1], F. Joseph Turk[1], Ziad Haddad[1], Sundararaman Gopalakrishnan[2], Tomislava Vukicevic[2], Zhuo Wang[3], P. Peggy Li[1], Brian. W. Knosp[1], Quoc A. Vu[1], and Bjorn H. Lambrigtsen[1]

[1] Jet Propulsion Laboratory, Pasadena, CA 91109
[2] Hurricane Research Division/AOML/NOAA, Miami, FL
[3] University of Illinois at Urbana-Champaign, Urbana, IL

1. Introduction

Currently there are still many unanswered questions about the physical processes that determine hurricane genesis and evolution. Furthermore, a significant amount of work remains to be done in validating and improving hurricane models. While the track forecast has improved significantly over the last couple of decades, the accuracy of the intensity forecast is still insufficient. As highlighted by the NOAA-led multi-agency Hurricane Forecast Improvement Project (HFIP), of particular importance is the need to improve our ability to forecast rapid intensification (RI) and weakening (RW) of tropical cyclones (TCs).

Recent studies indicate that the hurricane inner core processes and potential oceanic feedback might play a crucial role in determining the storm's intensity and size. Yet the understanding of these processes is still lacking. This brings to the forefront the need to better understand the role of the inner-core convective organization in TC intensity changes.

Recent studies have linked RI to intermittent occurrence of deep, strong convective bursts within the inner core (e.g. Hendricks et al., 2004; Montgomery et al., 2006; Rogers, 2010) occupying as little as 5–10% of the area of the hurricane eyewall. However, an alternative hypothesis is that RI follows abundant and well organized but weaker convection in the inner-core region (Gopalakrishnan et al., 2011). A continuous azimuthally symmetric eye wall (i.e., a ring) of precipitation then indicates the imminent onset of RI (Kieper and Jiang, 2012). This occurs when the ring is at least 90% closed and dominated by shallow warm precipitation extending from near the freezing level to the surface.

Our investigation employs a long record of satellite observations to address the questions above. The goal of our analyses is to learn how the 2D storm structure evolves and how it relates to the storm intensity and intensity changes with the objective to understand the underlying processes and to provide clues for model validation and improvement, as well as near-real-time predictive capability.

2. The JPL Tropical Cyclone Information System

Despite the significant amount of satellite observations today, they are still underutilized in hurricane research and operations, due to complexity and volume. To facilitate hurricane research, we developed the JPL Tropical Cyclone Information System (JPL TCIS) of multi-instrument satellite observations pertaining to: i) the thermodynamic and microphysical structure of the storms; ii) the air-sea interaction processes; iii) the larger-scale environment. The TCIS (http://tropicalcyclone.jpl.nasa.gov - Fig. 1) has two components: the Tropical Cyclone Data Archive - http://tropicalcyclone.jpl.nasa.gov/hurricane/gemain.jsp and the Interactive Data Portals (e.g. http://tropicalcyclone.jpl.nasa.gov/hs3).

The Tropical Cyclone Data Archive (Fig. 2) presents the satellite depiction of hurricanes over the globe during the period 1999-2011. It provides a one-stop place for fast access to both digital data (in NetCDF) and imagery, all subsetted to the domain and time of interest in order to decrease the amount of data for downloading. All this allows the users to obtain an extensive set of multi-parameter data from multiple observing systems, making the TCIS TC Data Archive a unique source to support hurricane research, forecast improvement and algorithm development.

3. Method

Following similar approaches (e.g. Lonfat et al., 2004, Rogers et al., 2012) we create a number of composites by aggregating satellite data from multiple storms as a function of their intensity, their intensification rate and their time-offset from the storms' maximum intensity time. Analyzing composites can be very helpful in revealing persistent structures. This approach allows the inclusion of cases with partial view of the storm that could not be analyzed individually. When building the composites we follow the approach of Wu et al. (2012) and develop the statistics for the four quadrants with respect to the storm motion (Fig. 3).

4. Asymmetry and its evolution as a function of storm category

Similarly to Lonfat et al. (2012) we first stratify the data into two intensity groups (Category 1-3 and Category 4-5). We then build composites using the storm-centric satellite observations available from the JPL TCIS.

4.1. Precipitation structure

a) The Rain Index

In this study we use multi-channel passive microwave observations (AMSR-E) to investigate the hurricane precipitation structure. In particular, we compute a Rain Index (Hristova-Veleva et al., 2013) that combines the emission and scattering signals from the multi-channel information (Fig. 4). Microwave signals at the top of the atmosphere can be classified into two categories: i) emission signal – it is a warming signal that is dominant at lower frequencies and is better suited for the depiction of light rain. Strong emission in the atmosphere reduces the polarization difference (PD) in the ocean surface radiation. Hence, PD is representative of the atmospheric emission; ii) scattering signal – a cooling signal that is dominant at higher frequencies. It is better suited for the depiction of heavy rain.

By incorporating both signals to cover the entire rainfall spectrum, the Rain Index presents a cohesive depiction of the rain and the graupel above. As Fig. 4 illustrates, the Rain Index shows a capability to depict small-scale features in the storm structure and to capture both regions of light precipitation as well as regions of heavy rain, thus providing information on the storm structure and a first-order estimate of the intensity of the precipitation. These features of the Rain Index make it a desirable tool to use in studying the distribution of precipitation in hurricanes. As already mentioned, the goal of our analyses is to understand how the 2D storm structure evolves and how it relates to the storm intensity and intensity changes.

b) The data

In this study we used nine years of AMSR-E observations of hurricanes in the North Atlantic. Using the Best Track data (also available from the JPL TCIS TC Data Archive) we first segregated the observations by the maximum intensity that was reached for a particular hurricane. We then combined all observations of storms from a particular category, organizing them in time bins as a function of the time of the observation relative to the time of maximum intensity. In doing so, we considered all observations within +-3 days of the storms' maximum intensity. The final number of cases we obtained is stratified as follows:

- Cat1 - 31 cases; Cat2 - 9 cases; Cat3 - 12 cases; **Total Cat1-3 = 52 cases**
- Cat4 - 18 cases; Cat5 - 7 cases; **Total Cat4-5 = 25 cases**

In our next step we will include observations from TMI, SSMI and SSMIS, all available from the JPL TCIS Data Archive. Making use of the observations from these multiple sensors will greatly increase the robustness of our statistics. Using the Rain Index as a proxy of the precipitation will also help significantly, as we will use the same measure of rain, being much less sensitive to uncertainty that arises from different instrument calibrations and from the use of different retrieval algorithms and assumptions.

c) Results

Results from the analysis of the precipitation structure are presented in Figures 5 and 6 which show the Rain Index value as a function of distance from storm center (y axis) and days from maximum intensity, marked as 0 on the x axis. The statistics were computed for each X and Y bin, separately for each of the four quadrants with respect to the storm motion and the results are presented in the four panels of each figure. Note that the higher the value of the Rain Index, the stronger the precipitation, as illustrated in Fig. 4. To assesses the storm asymmetry we compare the values of the Rain index in the four quadrants.

Let's first look at storms Cat 1-3 (Fig. 5). An inspection of the distribution of the Rain index in space and time shows that: i) more intense precipitation is found in ***the front*** (with respect to storm motion) ***two quadrants***; ii) the storm is most symmetric at the time of its maximum intensity; iii) after the peak of the storm there is a tendency for radial expansion of precipitation but it is limited to ***the front 2 quadrants*** only while the back two quadrants show a tendency for radial contraction (decrease of the area of precipitation). These opposing tendencies result in an increase in asymmetry, as indicated by the red arrows which show the trends in the evolution of the precipitation (area and intensity) within -3 to +3 days from maximum intensity.

The structure and evolution of the more intense storms (Cat 4-5, Fig. 6) is quite different. First, of course, these storms have more intense precipitation, as it should be expected and has been documented before (e.g. Lonefat et al., 2004). What is more interesting is that the stronger storms are: i) more compact; ii) more symmetric in both space and time.

4.2. Surface wind structure

We perform similar analyses, looking this time at the surface wind structure as depicted from 10 years of QuikSCAT scatterometer observations. In particular, we investigate the wind retrievals produced by our new *artificial neural network* (ANN) technique (Stiles et al., 2013) that provides reliable estimates of the surface winds under the rain and high-wind conditions typical for hurricanes, thus addressing long-standing issues of rain contamination inside the hurricane core. After performing the stratification by storm category we obtained the following number of storms:

- Cat1 - 38 cases; Cat2 -11 cases; Cat3 - 17 cases; **Total Cat1-3 = 66 cases**
- Cat4 - 21 cases; Cat5 - 7 cases; **Total Cat4-5 = 28 cases**

Figures 7 and 8 illustrate our results. Comparing the distributions for Cat 1-3 (Fig. 7) to these for Cat 4-5 (Fig.8) we find that for the weaker storms there is a lot of symmetry in space, and especially in time. This is in contrast to the precipitation structures for these storms (Fig. 5) that were characterized by significant asymmetry. On the other hand, the stronger storms (Cat4-5) show more asymmetry in space and especially in time. There is a tendency for radial expansion of the wind field after the peak of the storm and this tendency is more pronounced in ***the right two quadrants***, leading to increase in asymmetry with time.

To briefly summarize, while ***the precipitation fields for the weaker storms*** (Cat1-3) ***tend to be larger and more asymmetric than those for the stronger storms*** (Cat4-5), ***the wind fields show a reverse tendency, namely, the stronger storms are larger and more asymmetric***. The tendency for increase in asymmetry in time is manifested by: i) radial precipitation expansion in the front two quadrants for the weaker storms; and ii) radial wind expansion in the right two quadrants and for the stronger storms.

5. Storm asymmetry as a function of the Intensity Change Category.

As highlighted by the NOAA-led multi-agency Hurricane Forecast Improvement Project (HFIP), of particular importance is the need to improve our ability to forecast rapid intensification (RI) and weakening (RW) of tropical cyclones (TCs). With this goal in mind we next segregate the data in terms of the intensification rate of the storms. Listed below are the criteria we used in this study to define five categories in terms of their rate of intensity changes.

RW= Rapidly Weakening		DeltaSpeed	< - 4.75 m/s per 6hr (-37.0kt per 24h)
W= Weakening	-4.75 m/s per 6hr <	DeltaSpeed	< - 0.75 m/s per 6hr (- 5.8kt per 24h)
N= No change	-0.75 m/s per 6hr <	DeltaSpeed	< 2.25 m/s per 6hr (+17.5kt per 24h)
I= Intensifying	2.25 m/s per 6hr <	DelatSpeed	< 4.75 m/s per 6hr (+37.0kt per 24h)
RI= Rapidly Intensifying		DeltaSpeed	> 4.75 m/s per 6hr (+37.0kt per 24h)

Figure 9 shows the radial distribution of precipitation for each of the storm intensity change categories we defined and for the four quadrants wrt storm motion that we used before (shown in the four panels). Distance from storm center is presented on the y axis in each of the four panels. The x axis presents now the category of the storm intensity change, spanning the five categories from RW (Rapidly Weakening) on the left side of the x axis and the RI (Rapidly Intensifying) on the right side of the axis. Figure 10 shows the same statistics but computed for the radial distribution of the scatterometer-derived surface wind field.

Inspection of the results in Figures 9 and 10 reveals that:

- Rapidly Intensifying storms have most symmetric wind and rain fields
- Rapidly Weakening storms have most asymmetric wind and rain with:
    - Stronger rain in the 2 forward quadrants
    - Stronger wind in the 2 right quadrants
- Intensifying and Weakening storms are similar in asymmetry with the Intensifying storms being somewhat stronger
- Neutral storms have the weakest fields

6. Summary

To facilitate hurricane research, we developed the JPL Tropical Cyclone Information System (TCIS) of multi-parameter multi-instrument observations (satellite, airborne and in-situ) pertaining to: i) the thermodynamic and microphysical structure of the storms; ii) the air-sea interaction processes; iii) the larger-scale environment.

One of the two main components of the JPL TCIS is an archival database of satellite observations (http://tropicalcyclone.jpl.nasa.gov/hurricane/gemain.jsp). The TC Data Archive presents the satellite depiction of hurricanes over the globe during the period 1999-2011. It offers both data and imagery that are subsetted to the domain and time of interest.

The TC Data Archive was developed to help reduce the amount of time for discovery of data across different NASA data archives and to decrease the amount of data to download in order to develop robust statistical analysis. The TC Data Archive provides a one-stop place to obtain an extensive set of multi-parameter data from multiple observing systems, making it a unique source to support hurricane research, forecast improvement and algorithm development.

In this study we used data from the TC Data Archive. In particular, we analyzed the rain and wind fields of the Atlantic hurricanes during the last decade. We used two new products to perform our analysis. As a proxy for the rain field we studied the distribution of the Rain Index – a multi-channel passive microwave signal (Hristova-Veleva et al., 2013) we computed from the observations of AMSR-E. To study the spatial and temporal distribution of the surface winds we used a new hurricane–specific surface wind product (from QuikSCAT) that provides reliable wind estimates under rain and in high-wind conditions typical for hurricanes.

We investigated two aspects of the hurricane structure:

- the storm **asymmetry and its evolution** as a function of storm intensity (Cat1-3 versus Cat4-5)
- the **storm asymmetry and its relationship to the rate of storm intensity changes** which we broke down into five categories:
    - **R**apidly **W**eakening, **W**eakening, **N**eutral, **I**ntensifying, **R**apidly **I**ntensifying

We find that:

- Category 1-3 hurricanes show different evolution of the storm asymmetry than Cat 4-5.
- Rain and Wind fields show different evolution of the asymmetry
    - **Rain: Cat 1-3 fields are larger and less symmetric in both space and time (**more intense precipitation is in the **front 2 quadrants**; Radial expansion of precipitation after the storm peak (**front 2 quadrants**). Increase in asymmetry
    - **Wind: Cat 4-5 fields are larger and less symmetric in both space and time** (stronger winds in the **right 2 quadrants**; Radial expansion of high winds after the peak of the storm. More pronounced in the **right 2 quadrants**; Increase in asymmetry)
    - Of course, in both cases (rain and wind) Cat4-5 have more intense fields.
- Rapidly Intensifying (**RI**) and Rapidly Weakening (**RW**) storms show structures that make them distinguishable from the other storms.
    - **RI storms have most symmetric wind and rain fields**
    - **RW storms have most asymmetric wind and rain with:** Stronger rain in the 2 forward quadrants; Stronger wind in the 2 right quadrants

To summarize, here we presented the results of our analysis of the 2D rain and wind structure and related them to the storm intensity and intensification rates with the goal to understand the underlying processes and to provide clues for model validation and improvement, as well as near-real-time predictive capability. By employing a 12-year long record of global satellite observations we are able to extract statistically-robust signatures of the importance of the storm organization. By looking at the statistics of multiple variables (rain and wind) we develop a more complete view of the storm structure and evolution.

7. Future plans

We plan to extend our current study to include 13+ years of observations from a number of different instruments (TMI, SSMI/SSMIS and the recently launched GMI) in addition to the current study of AMSR-E observations. As we pointed out before, our use of the Rain Index will be very beneficial since we can compute it with very similar accuracy from all these instruments (only the lower spatial resolution of the SSMI and SSMIS observations would introduce some inconsistency, but it is not expected to be too significant). Furthermore, we will include additional scatterometer surface wind retrievals from OSCAT observations using the same ANN retrieval algorithm as in the current QuikSCAT retrievals.

By expanding the set of available observations we should be able to further break down the groups by storm category, time from peak intensity, and storm intensification rate. What we really hope to do is to be able to distinguish between rapidly intensifying, intensifying, neutral, weakening and rapidly weakening storms – the distinction being based on the rain and wind structures and their evolution prior the rapidly intensifying stage.

Looking at the long-term statistics from multiple instruments and multiple variables will provide a more complete view of the storm structure and evolution, with the hope to obtain better predictive skills.

Acknowledgments:

The work described here was performed at the Jet Propulsion Laboratory, California Institute of Technology, under contract with the National Aeronautics and Space Administration. This work was supported by two NASA grants: NASA grant NNH08ZDA001N –HSRP and NASA/ESTO grant NNH11ZDA001N-AIST. We also acknowledge the support from several JPL programs (Innovative Spontaneous Concepts R&TD and SURP) and satellite projects (AISR, QuikSCAT, CloudSAT and MLS).

References:

Gopalakrishnan, S.G., F. Marks, X. Zhang, J.-W. Bao, K.-S. Yeh, and R. Atlas, 2011: The Experimental HWRF system: A study on the influence of horizontal resolution on the structure and intensity changes in tropical cyclones using an idealized framework. Monthly Weather Review,139(6):1762-1784 (doi:10.1175/ 2010MWR3535.1).

Hendricks, E.A., M.T. Montgomery, and C.A. Davis, "The role of 'vortical' hot towers in the formation of Tropical Cyclone Diana (1984)." J. Atmos. Sci., vol. 61, pp. 1209–1232, 2004.

Hristova-Veleva, S. M., P. S.Callahan, R. S. Dunbar, B. W. Stiles, S. H. Yueh, J. N. Huddleston, S. V. Hsiao, G. Neumann, M. H. Freilich, B. A. Vanhoff, W.Y. Tsai, R. W. Gaston, E. Rodriguez and David E. Weissman, 2013: "Revealing the Winds Under the Rain. Part I. Passive Microwave Rain Retrievals Using a New, Observations-Based, Parameterization of

Sub-Satellite Rain Variability and Intensity: Algorithm Description", Journal of Applied Meteorology and Climatology, in press.
Kieper, M. E., and H. Jiang, 2012: Predicting tropical cyclone rapid intensification using the 37 Ghz ring pattern identified from passive microwave measurements,Geophys. Res. Lett., 39, L13804, doi:10.1029/2012GL052115.
Lonfat, M., F.D.MARKS, and S.S.Chen, 2004: "Precipitation Distribution in Tropical Cyclones using the Tropical Rainfall Measuring Mission (TRMM) microwave imager : A Global Perspective" Mon.Wea.Review 132(7) p.1645-1660 (July 2004)
Montgomery, M.T., M.E. Nicholls, T.A. Cram, and A. Saunders, "A 'vortical' hot tower route to tropical cyclogenesis." J. Atmos. Sci., vol. 63, pp. 355–386, 2006.
Rogers, R.F., "Convective-scale structure and evolution during a high-resolution simulation of tropical cyclone rapid intensification." J. Atmos. Sci., vol. 67, pp. 44–70, 2010.
Rogers, R., S. Lorsolo, P. Reasor, J. Gamache, and F. D. Marks, 2012: "Multiscale analysis of mature tropical cyclone structure from airborne Doppler composites," Monthly Weather Review, 140 (1), P. 77-99 (January 2012)
Stiles, B.W., R. E. Danielson, W. Lee Poulsen, Michael J. Brennan, Svetla Hristova-Veleva, Tsae-Pyng J. Shen, and Alexander G. Fore, "Optimized Tropical Cyclone Winds from QuikSCAT: A Neural Network Approach," submitted to IEEE TGARS, 2013.
Wu, L, H. Su, R. G. Fovell, B. Wang, J. T. Shen, B. H. Kahn, S. M. Hristova-Veleva, B. H. Lambrigtsen, E. J. Fetzer, J. H. Jiang, 2012: "Relationship of Environmental Relative Humidity with Tropical Cyclone Intensity and Intensification Rate over North Atlantic", Geophys. Res. Lett., 39, L20809, doi:10.1029/2012GL053546.

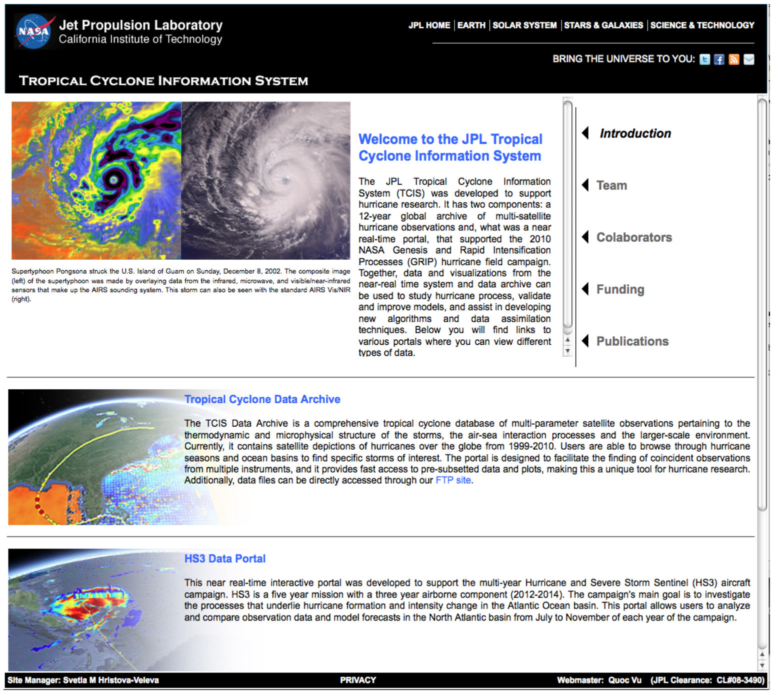

Figure 1. Front page of the JPL Tropical Cyclone Information System (http://tropicalcyclone.jpl.nasa.gov). It provides an overview of the goals and serves as a gateway to the two main components of the system: the TCIS Tropical Cyclone Data Archive; and the set of Interactive Portals (HS3 and GRIP) that combine satellite observations with model forecast to allow interrogation of a large set of parameters and comparisons between models and observations. As their names suggest, these interactive portals were run in support of two recent hurricane field campaigns – GRIP (2010) and HS3 (2012-2015)

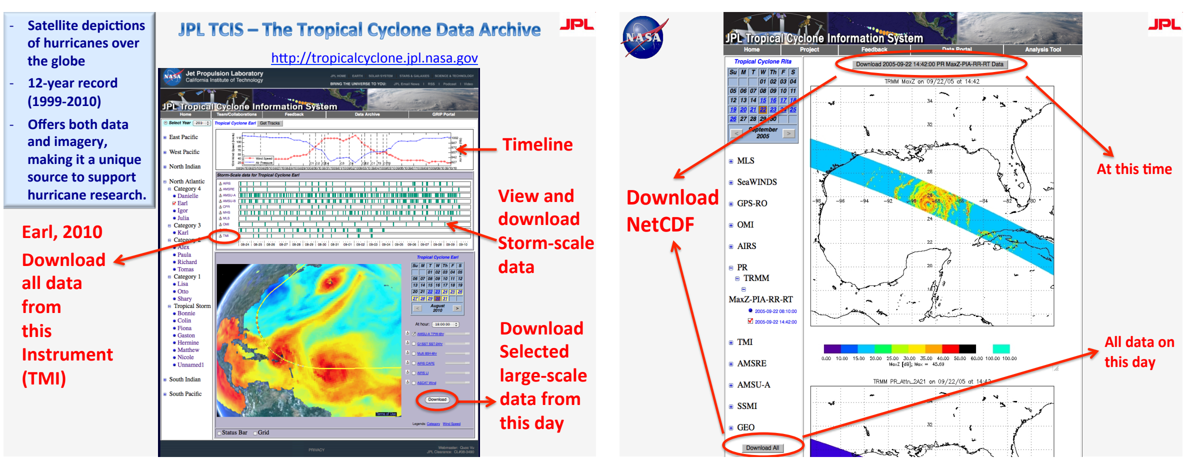

Figure 2. Left panel shows the front page of the JPL TCIS Tropical Cyclone Data Archive (http://tropicalcyclone.jpl.nasa.gov/hurricane/gemain.jsp) while the right panel illustrates an example of the storm-specific second page which presents data from the instruments of interest that are subsetted to to 2000x2000 km domain centered on the time-interpolated "Best Track" location. Digital data (in NetCDF format) and the associated imagery can be downloaded from either of those web pages.

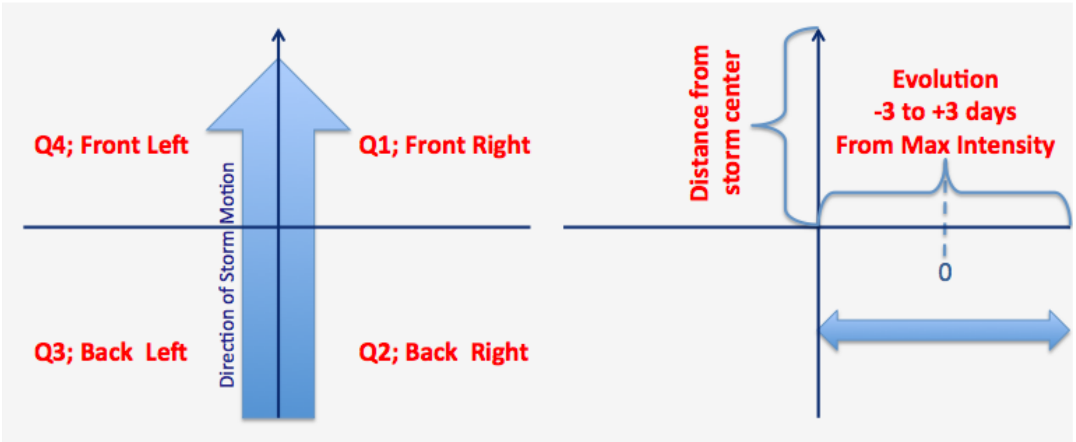

Figure 3. Schematic illustrating the approach to developing the composites by segregating the observations in bins that reflect: the track-relative storm structure (the quadrants for which statistics are presented in the four panels); the radial distance from the storm center (y axis in each of the four panels); and the difference (in days) from the time of maximum intensity (x axis in each of the four panels).

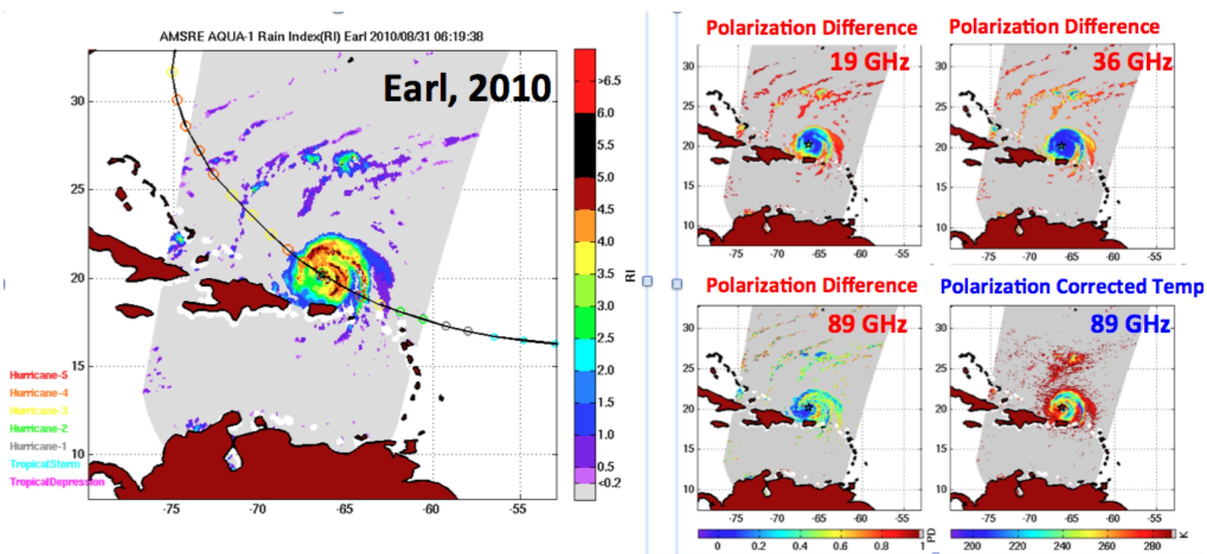

Figure 4. Rain index (left panel) and components (right panel) as computed from AMSR-E observations of hurricane Earl (2010). By combining information from multiple channels, through the use of the various emission and scattering signals, the Rain Index shows a capability to depict small-scale features in the storm structure and to capture both regions of light precipitation as well as regions of heavy rain, thus providing information on the storm structure and first-order estimate of the intensity of the precipitation.

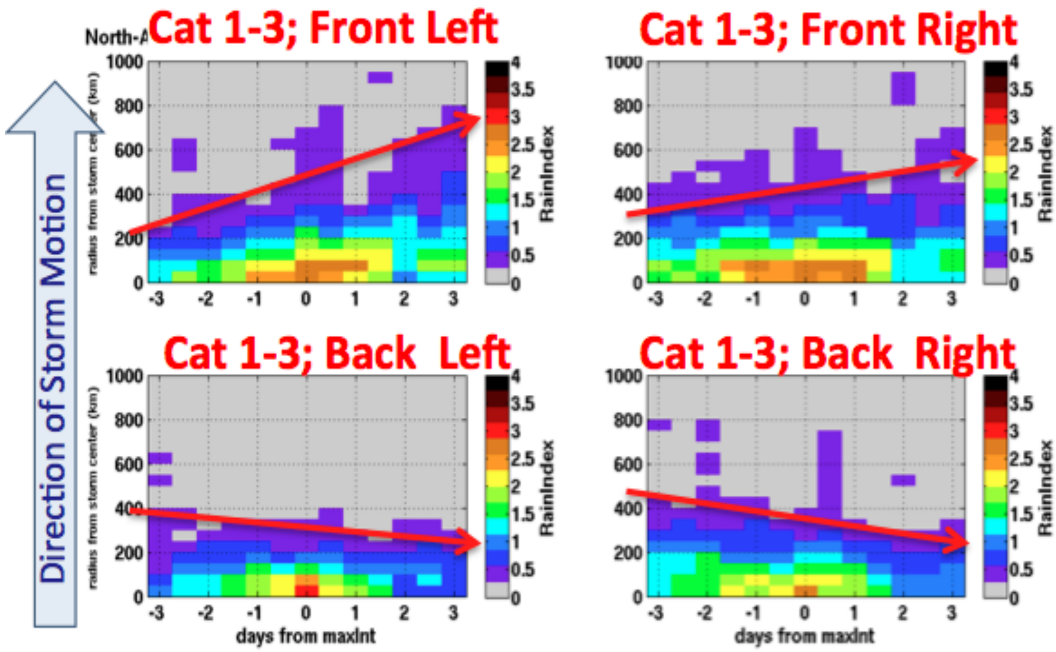

Figure 5. Distribution of precipitation, as depicted by the Rain Index. The statistics were computed from 9 years of AMSR-E observations of North Atlantic hurricanes that reached maximum intensity of Category 1-3. In each of the four plots, the X axis shows days from maximum intensity, marked as 0, while the Y axis shows distance from storm center, in 50km bins. The mean Rain Index is computed for each X and Y value, separately for each of the four quadrants with respect to the storm motion and the results are presented in the four panels. The red arrows indicate the trends in the evolution of the precipitation (area and intensity) within -3 to +3 days from maximum intensity.

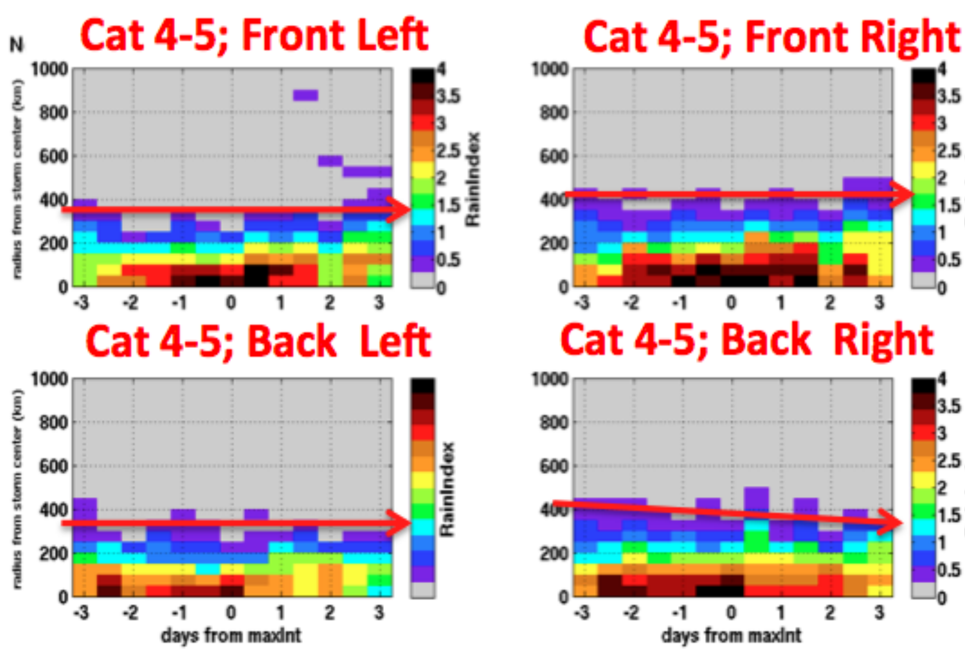

Figure 6. Same as figure 5 but for statistics built from storms that reached Category 4 and 5.

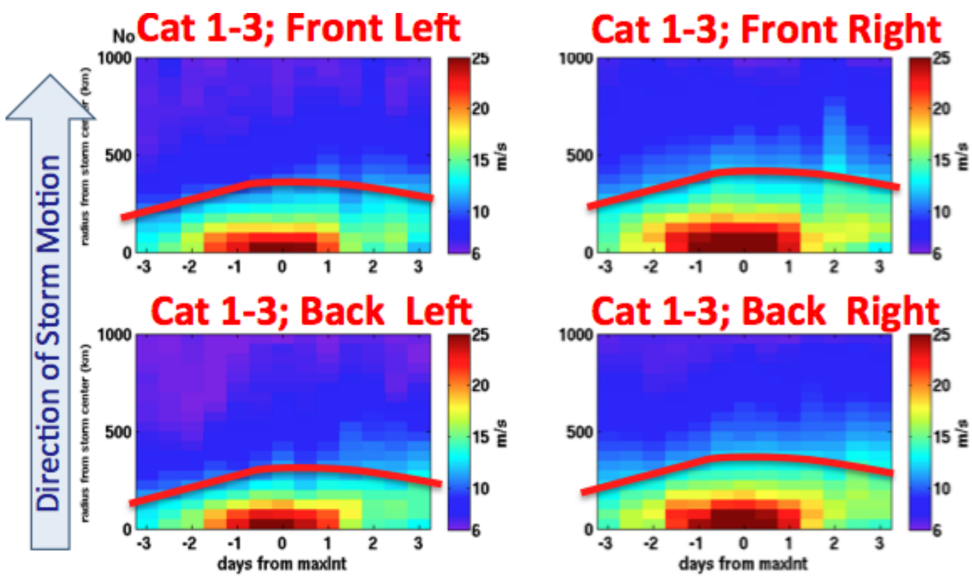

Figure 7. Same as in Fig. 5 except from the statistics are computed using scatterometer wind estimates obtained from 10 years of QuikSCAT observations. The retrieval were performed using a new ANN algorithm that allows much improved surface wind estimates under precipitation and in high wind conditions that are typical for hurricanes.

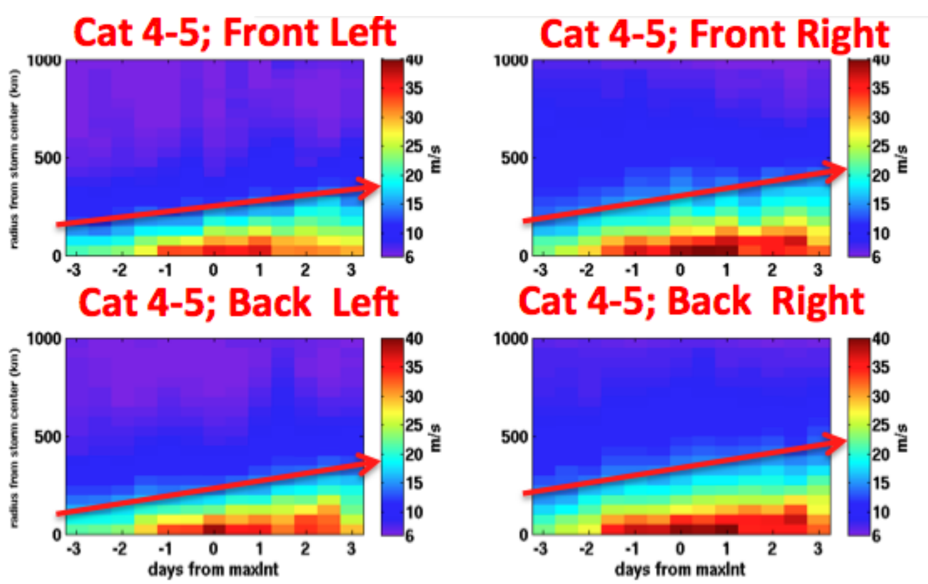

Figure 8. Same as in Fig. 6 except for using scatterometer surface wind estimates as in Fig. 7.

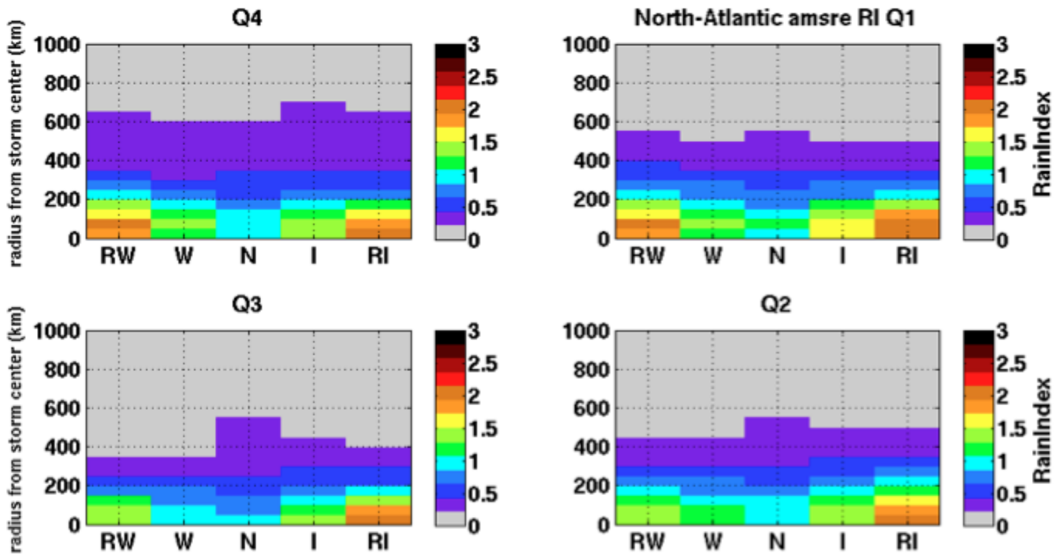

Figure 9. Radial distribution of precipitation for each of the storm intensity change categories we defined and for the four quadrants wrt storm motion that we used before (shown in the four panels). Distance from storm center is presented on the y axis in each of the four panels. The x axis presents now the category of the storm intensity change, spanning the five categories from RW (Rapidly Weakening) on the left side of the x axis and the RI (Rapidly Intensifying) on the right side of the axis.

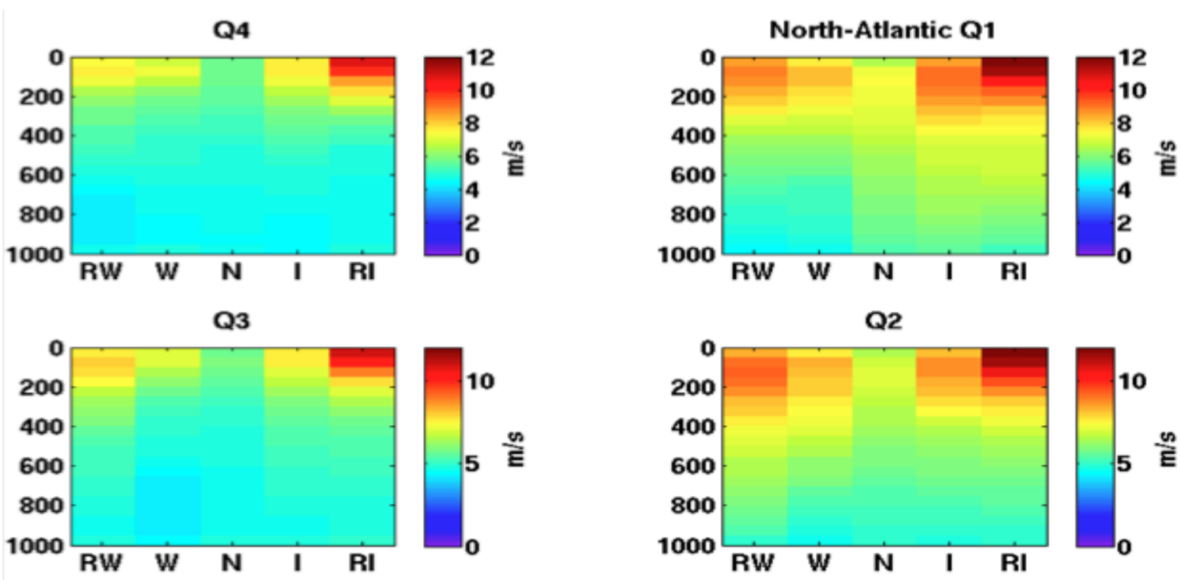

Figure 10. Same as in Fig.9 except for presented is the distribution of the scatterometer-derived surface winds. Note that now the radial distance increases top to bottom.